Am J Cancer Res 2017;7(3):673-687
www.ajcr.us /ISSN:2156-6976/ajcr0043060

Original Article

Control of tissue size and development by a regulatory element in the *yorkie* 3'UTR

Takanari Umegawachi[1*], Hideki Yoshida[1,2*], Hiromu Koshida[1], Momoko Yamada[1], Yasuyuki Ohkawa[3], Tetsuya Sato[3], Mikita Suyama[3], Henry M Krause[4,5,6], Masamitsu Yamaguchi[1,2]

[1]Department of Applied Biology, [2]The Center for Advanced Insect Research Promotion, Kyoto Institute of Technology, Matsugasaki, Sakyo-ku, Kyoto 606-8585, Japan; [3]Medical Institute of Bioregulation, Kyushu University, Fukuoka 812-8582, Japan; [4]Banting and Best Department of Medical Research, [5]Department of Molecular Genetics, [6]Donnelly Centre, University of Toronto, Toronto, Ontario M5G 1L6, Canada. [*]Equal contributors.

Received October 28, 2016; Accepted October 31, 2016; Epub March 1, 2017; Published March 15, 2017

Abstract: Regulation of the Hippo pathway via phosphorylation of Yorkie (Yki), the *Drosophila* homolog of human Yes-associated protein 1, is conserved from *Drosophila* to humans. Overexpression of a non-phosphorylatable form of Yki induces severe overgrowth in adult fly eyes. Here, we show that *yki* mRNA associates with microsomal fractions and forms foci that partially colocalize to processing bodies in the vicinity of endoplasmic reticulum. This localization is dependent on a stem-loop (SL) structure in the 3' untranslated region of *yki*. Surprisingly, expression of SL deleted *yki* in eye imaginal discs also results in severe overgrowth phenotypes. When the structure of the SL is disrupted, Yki protein levels increase without a significant effect on RNA levels. When the SL is completely removed, protein levels drastically increase, but in this case, due to increased RNA stability. In the latter case, we show that the increased RNA accumulation is due to removal of a putative *miR-8* seed sequence in the SL. These data demonstrate the function of two novel regulatory mechanisms, both controlled by the *yki* SL element, that are essential for proper Hippo pathway mediated growth regulation.

Keywords: *yki* mRNA, mRNA localization, hippo pathway

Introduction

The Hippo pathway is highly conserved signaling pathway from *Drosophila* to humans. The Hippo pathway regulates tissue size and defect in the pathway leads to tissue overgrowth [1, 2]. Yorkie (Yki) and its mammalian homolog Yes-associated protein (YAP) are essential components of the Hippo pathway and can activate the expression of genes related to cell proliferation and anti-apoptosis. The activity of Yki and YAP1 is negatively regulated by phosphorylation through the Hippo signaling pathway. In *Drosophila*, overexpression of non-phosphorylatable Yki by substitution mutation into phosphorylation site but not wild-type Yki in the eye imaginal discs induces severe overgrowth phenotype in adult compound eyes [3]. While mutation at phosphorylation sites of YAP1 has not been found in human cancer patients, the amplification of genomic region containing the *YAP1* gene and overexpression of YAP1 are reported in human and mouse tumors [4-6]. Although it is suggested that perturbation of the regulation by microRNAs leads to up-regulation of *YAP1* gene expression in tumors [7], most of the mechanisms underlying YAP1 overexpression in tumors are still unclear.

It is well known that mRNAs encoding secreted or membrane proteins, upon translation, are targeted to the endoplasmic reticulum (ER) in a signal recognition particle (SRP)-dependent manner [8-10]. Recently, however, genome-wide analyses have suggested that many of these mRNAs, as well as many other mRNAs that encode nuclear and cytosolic proteins, are also targeted to the ER in a translationally-independent fashion [11-15]. In several cases, cis-elements and trans-factors that are related to this SRP-independent ER targeting have been identified [16, 17]. However, because the bio-

logical significance of this ER targeting is still unclear, we attempted to develop a *Drosophila* model that is able to connect these observations with *in vivo* biological functions.

In this paper, we identify *yki* mRNA encoding transcriptional co-activator as one of the mRNAs fractionated into microsome fraction in SRP-independent manner and reveal that *yki* mRNA localizes to processing bodies (P-bodies), which is dependent on a stem-loop (SL) structure in its 3' untranslated region (UTR). Furthermore, we indicate that the SL is related to two distinct regulations of *yki* gene expression at mRNA level and expression of the SL-deleted *yki* in the eye imaginal discs results in severe overgrowth phenotype in the adult compound eyes.

Materials and methods

DNA constructs

NLS-MCP-GFP was amplified from pCaSpeR-hsp83-NLS-MCP-GFP [18], and inserted into the TA cloning vector pCR2.1 (Invitrogen). The NLS-MCP-GFP was removed from pCR2.1-NLS-MCP-GFP by digesting with *Bgl*II and *BamH*I, and cloned into the *Bgl*II/*BamH*I site of pCaSpeR-hs/act.

ms2 × 12 was isolated from vector pCR-ms2 × 12 using *Bgl*II/*BamH*I, and inserted into the vector pMT/V5-HisB (Invitrogen). *Escherichia coli* TOP10 was used for constructing all recombinant plasmids containing ms2 sequences. Transformed TOP10 was then spread onto LB plates containing carbenicillin, and incubated at 30°C for 17 h.

To generate an ER maker, the signal sequence (ss) of *Calreticulin* (*Crc*), and HDEL coding sequences, were inserted into the *Not*I/*BamH*I site of pAc5.1/V5-HisA. DsRed was amplified from pDsRed-Monomer (Clontech) and inserted between the ss and HDEL sequence using the *Xba*I site of pAc5.1-ss-HDEL. The *Vm34Ca*, *Act5C* and *yki* sequences were amplified from cDNA synthesized from total RNA of S2-DRSC cells (DGRC), and cloned into pMT/V5-HisB-ms × 12 using the *Xho*I site and the In-fusion HD cloning kit (TaKaRa Clontech).

To make a P-body marker, *Me31B* was amplified from an EST clone (LD21247), and inserted into the pDsRed-Monomer vector. *Me31B*-DsRed was amplified from p*Me31B*-DsRed, and inserted into the *Xho*I/*Mlu*I sites of pAc5.1/V5-HisA.

Deletion constructs or mutants of *yki* were amplified from pMT-*yki*-ms2 × 12, and inserted into the *Xho*I site of pMT/V5-HisB-ms2 × 12.

Plasmids for the expression of *miR-8* primary transcripts and miRNA reporters have been described previously [19, 20]. The *YAP1* 3'UTR was amplified from cDNA synthesized from total RNA of HEK293 cells. The *yki* 3'UTR, *yki* 3'UTR mutants, and *YAP1* 3'UTR were then inserted into a *sty*I site that is in the 3'UTR of the firefly luciferase reporter in pGVB using the In-fusion HD cloning kit. The *miR-8* expression and reporter plasmids contain an *Actin 5C* promoter.

To make plasmids for dsRNA of *lacZ*, *Srp54k*, *AGO1*, and *HPat-1*, each gene was amplified from a pMT/V5-His/lacZ vector, or cDNA synthesized from total RNA of S2-DRSC cells, and cloned into pOT2 using the *Xho*I and *EcoR*I sites.

Cell culture and RNAi

S2-DRSC cells were maintained at 25°C in Schneider's *Drosophila* medium (Life technologies™) supplemented with 10% fetal bovine serum (FBS), 50 units/ml penicillin (Invitrogen), 50 μg/ml streptomycin (Invitrogen) and 0.1 mg/ml gentamicin (Life technologies™).

RNAi was performed as described [21]. dsRNA was synthesized from linearized pOT2 vectors using T7 and SP6 polymerases and RiboMAX™ expression large scale RNA production kit (Promega) according to the manufacturer's protocol.

S2-DRSC cells were plated into 24-well plates with 2.5 × 10^5 cells in 450 μl of medium supplemented with 10% heat-inactivated FBS, penicillin, streptomycin and gentamicin per well. After plating, 1 μg of dsRNA was transfected using DharmaFECT4 transfection reagent (GE Dharmacon). After 24 h, knockdown cells were transfected with plasmids for RNA imaging and luciferase assays.

Cell fractionation

5.0 × 10^8 S2-DRSC cells were collected by centrifugation (1,000 × g, 5 min), frozen with liquid N_2 and resuspended in 5 mL HKM buffer containing 30 mM HEPES [pH 7.3], 50 mM KCl, 2.5

mM $MgCl_2$, 0.88 M sucrose, 1 mM DTT and complete-mini [EDTA-free] protease inhibitors (Roche). The cells were homogenized with 30 strokes in a 21-gauge needle on ice. Nuclei and cell debris were removed by sedimentation at 1,000 × g for 20 min at 4°C, and the supernatant (S1) was further centrifuged at 10,000 × g for 30 min at 4°C to separate into pellet (P10) and supernatant (S10). P10 pellet resuspended in HKM buffer, and the S10 fraction, were loaded onto discontinuous sucrose gradients containing 1.3 M, 2.1 M and 2.7 M sucrose, followed by centrifugation at 190,000 × g for 4 h at 4°C in a RPS40T rotor (HITACHI). After centrifugation, the gradient solutions were withdrawn from the bottom of the tubes through a hole opened by needle to generate 3-drops fractions (~150 µl). Fractions were analysed by UV spectrometry and Western blotting.

Detachment of ribosomes from rough ER

Ribosome removal from rough ER was performed by treatment with puromycin in high-salt buffer [22]. 50 µl of RM fraction was diluted 11-fold with Stripping buffer containing 1 M KCl, 50 mM EDTA, 1 mM DTT, 30 mM HEPES, 1 mM puromycin, and incubated at 37°C for 30 min, then centrifuged at 75,000 × g for 10 min in a RPS40T rotor (HITACHI) at 4°C to produce a naked microsome (NM) pellet and stripped ribosome (SR) supernatant. The membrane pellet was then resuspended in HKM buffer and subjected to Western blot analysis.

RNA FISH and immunofluorescence

RNA *in situ* hybridization was carried out essentially as described previously [23]. 1×10^5 S2-DRSC cells were plated per well on an 8-well culture Slide (BD Falcon™), and incubated at 25°C for 3 days with 100 µg/ml Gentamycin. 3 µg/ml proteinase K treatment was performed at 4°C for 3 min. For hybridization, DIG-labeled probes were diluted in hybridization buffer at a concentration of 1 µg/ml, and incubated for 16 h at 45°C.

For probe detection, cells were incubated with Biotin-conjugated anti-DIG antibody (Roche: 1: 400 dilution) at 25°C for 1.5 h. Streptavidin-HRP secondary antibody (Perkin Elmer life sciences: 1:500 dilution) was incubated at 25°C for 30 min. To amplify signals, FITC-tyramide (1:50 dilution) was incubated at 25°C for 2 h. Following tyramide amplification, cells were fixed with 4% paraformaldehyde in HCMF at 25°C for 10 min, and blocked with 5% normal goat serum (Vector Labs) for 5 min. Cells were incubated for 16 h at 4°C with primary antibody, and then stained with Alexa Fluor 594-conjugated secondary antibody (Molecular Probes: 1:400 dilution) at 25°C for 1 h. Samples were mounted with VECTASHIELD mounting medium with DAPI (Vector Labs). Confocal images were obtained with a Fluoview FV10i confocal microscope, and analysed with MetaMorph software.

RNA imaging

2.5×10^5 cells were plated per well of a 24-well cell culture dish, and grown for 24 h. S2-DRSC cells were transfected with the pCaSpeR-hs-MCP-GFP, the *Drosophila* expression vector pMT-target RNA-ms2 × 12, pAc5.1-Sp-DsRed-HDEL or pAc5.1-*Me31B*-DsRed using siLentFect™ lipid reagent (Bio-Rad). After 24 h, cells were heat-shocked at 37°C for 30 min twice with 30 min interval at 25°C to induce MCP-GFP protein. Following heat shock, target RNA was induced by the addition of 500 µM $CuSO_4$ for 24 h. Images were captured using Fluoview FV10i confocal microscope (Olympus) and analysed with MetaMorph software (Molecular devices).

Generation of stable S2-DRSC cell lines

Stable line generation was as previously described [24]. 5×10^5 cells were plated per well in a 24-well cell culture dish, grown for 24 h and transfected with 400 ng pAc5.1-*miR-8*, together with 10 ng pCoBlast plasmid using siLentFect™ lipid reagent (Bio-Rad). Two days after transfection, cells were collected and incubated in medium containing 1 µg/ml Blasticidin S (Life Technologies), with changes every 4 days over several weeks. Total RNA was isolated for quantitative real-time PCR.

RNA-seq analysis

3 µg Total RNA of RM, cytoplasm, NM, and SR fraction were isolated using TRIzol Reagent (Invitrogen). Isolated RNAs were used for library construction with TruSeq RNA Sample Prep Kit (Illumina) according to the manufacturer's instructions. All samples were sequenced by illumine Genome Analyzer IIX with 41 bp single-end reads. The deep sequencing data were mapped to the reference *D. melanogaster* genome sequence (UCSC version dm3) by the

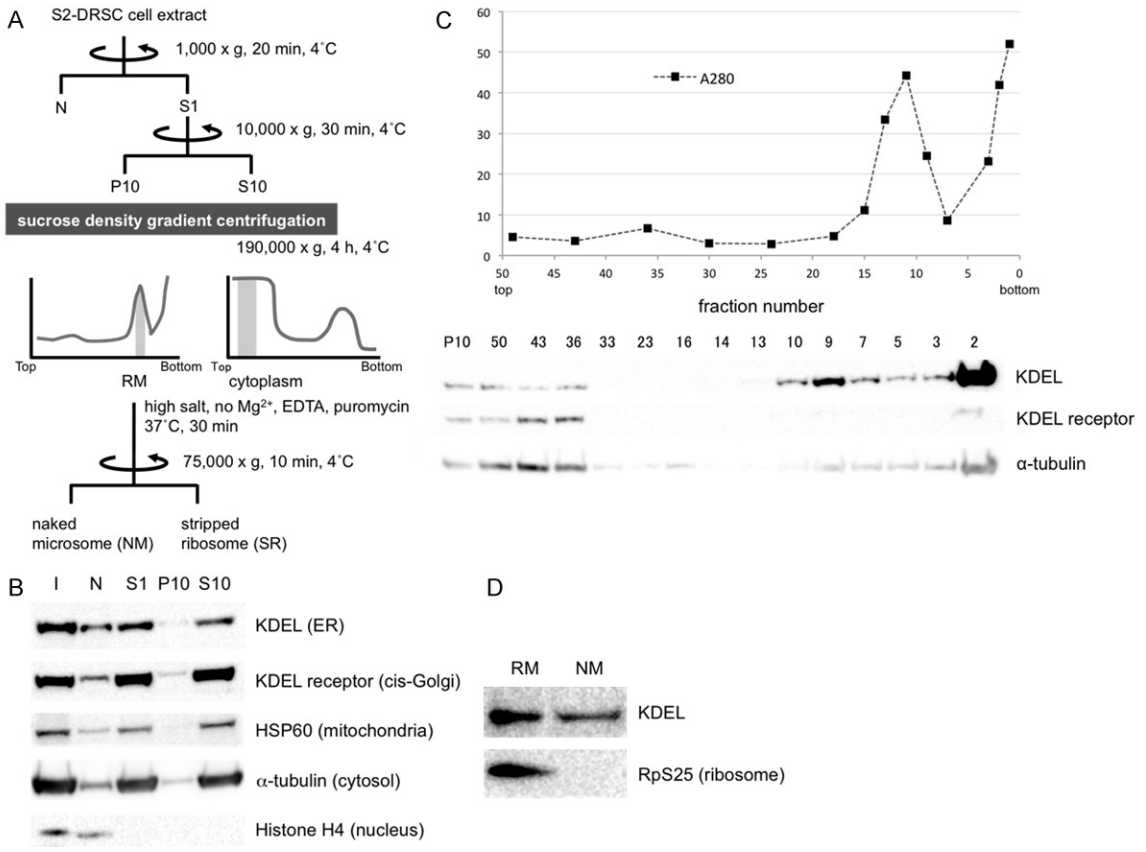

Figure 1. Rough microsomal (RM), cytoplasm (C), naked microsome (NM) and stripped microsome (SR) fractions were purified from S2-DRSC cells to identify mRNAs targeted to ER in an SRP-independent manner. A. Scheme for isolation of RM, C, NM and SR fractions. Shaded regions in the graphs indicate fractions that gave rise to the RM and C pools. B. After fractionation, organelle distributions were determined by Western blot analysis with anti-KDEL (ER), KDEL receptor (cis-Golgi), HSP60 (mitochondria), a-tubulin (cytosol) and Histone H4 (nucleus) antibodies, respectively. I = input. C. P10 fraction by sucrose density gradient centrifugation. The graph shows total protein levels detected by UV spectrometry, and the Western blot below illustrates the separation of ER and Golgi. D. Ribosomes on ER-containing fractions were stripped by treatment with EDTA and puromycin in high salt buffer. As expected, the ribosomal marker RpS25 detected by Western blot analysis is no longer detected in the NM fraction.

TopHat [25] program version 1.3.2 with default parameters. The Cufflinks [26] program version 2.0.0 was then used to assemble transcripts and to calculate fragments per kilobase of transcript per million mapped fragments (FPKM) with option '-library-type fr-secondstrand'. All results have been submitted to the Gene Expression Omnibus database (Accession number: GSE85768).

Statistical analysis

All statistical analyses, including Student's t tests, and ANOVA were performed using GraphPad Prism software.

Quantitative real-time PCR

Total RNA was extracted from intact S2-DRSC cells, cell fractions or the eye imaginal discs using Trizol (Invitrogen) and Dr. GenTLE precipitation carrier (TaKaRa). Total RNA was treated with DNaseI in DNase Buffer containing 40 mM Tris-HCl [pH 8.0], 8 mM $MgCl_2$, 1 mM $CaCl_2$ and 5 mM DTT at 37°C for 30 min. cDNA was synthesized from total RNA using a PrimeScript™ RT kit (Perfect Real Time, TaKaRa). Real time PCR primers were designed using the IDT Primer Quest Tool. Real-Time PCR was performed using SYBR® Premix Ex Taq™ II (Tli RNaseH Plus, TaKaRa), and analysed using the CFX96 Touch™ Real-Time PCR detection system (Bio-Rad). *Srp54k, yki, HPat-1AGO1*, *RpL32* and *spi* mRNA expressions were normalised to levels of *GAPDH* mRNA.

Luciferase assays

2.5×10^5 cells were plated per well of a 24-well cell culture dish and grown for 24 h. Transfection

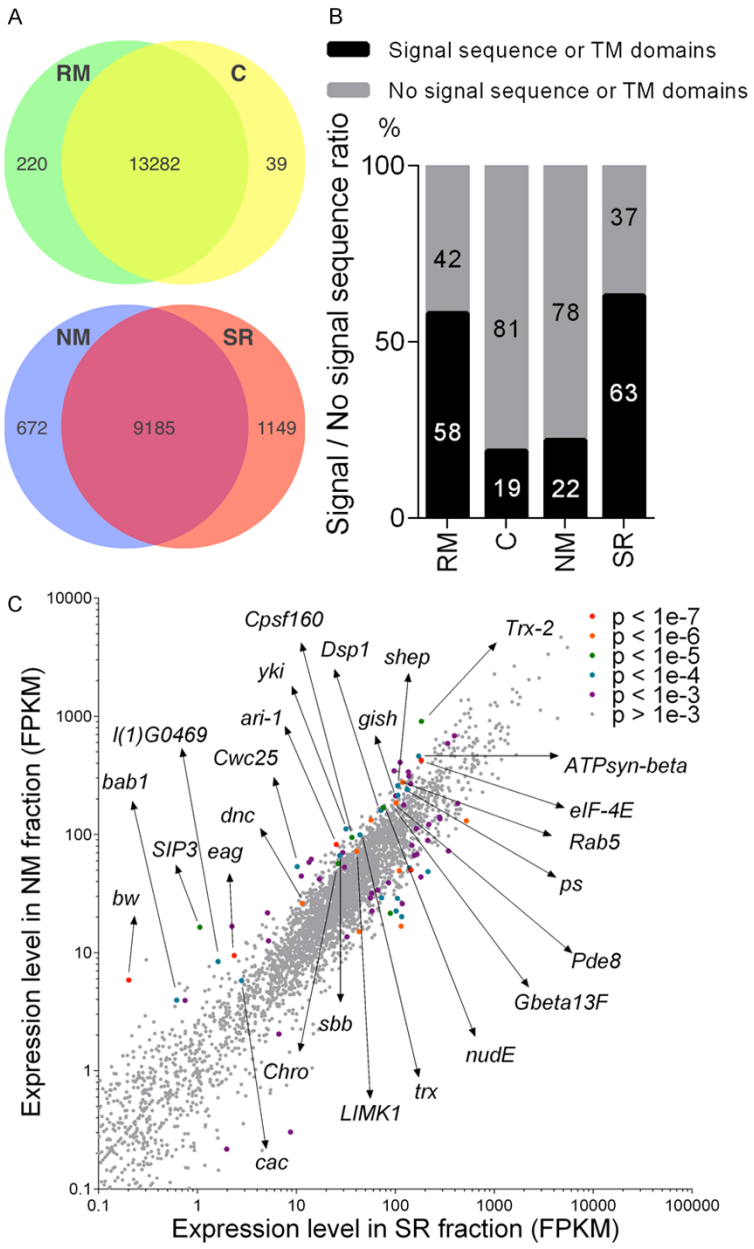

Figure 2. RNA-seq analysis of mRNAs in RM, C, NM or SR fractions. A. Numbers of identified mRNAs in RM, C, NM and SR, respectively. Similar numbers of transcripts were detected in the RM and C fractions and within the NM and SR fractions. B. The percentage of mRNAs bearing signal sequences (black bar) or not (gray bar) in the 200 most highly enriched transcripts in each fraction. C. Scatter plot showing that mRNAs encoding numerous types of proteins are enriched in NM. All analyses were carried out by using the GSE85768 dataset.

was performed in 24-well dishes using siLentFect™ lipid reagent (Bio-Rad). The following plasmids were cotransfected: firefly luciferase reporter gene construct (0.1 μg), pRL-SV40 Renilla luciferase (0.01 μg, transfection control plasmid), and either pAc5.1-*miR-8* or pAc5.1 empty vector (1 μg).

Dual Luciferase assays were performed 2 days after transfection according to the manufacturer's protocol (Promega), and total RNA was isolated for quantitative real-time PCR. *F-luc* mRNA levels were normalised to *R-luc* mRNA.

Antibodies

Antibodies used in this study are listed below in the format of name; application; supplier; catalogue; fold dilution. Mouse anti-KDEL; Western, Immunostaining; stressgen; 10C3; 1:2,000 dilution, 1:200 dilution. Mouse anti-α-tubulin; Western; Sigma; T5168; 1:8,000 dilution. Rabbit anti-GM-130; Western; abcam; ab30-637; 1:1,000 dilution. Mouse anti-HSP60; Western; Enzo; ADI-SPA 806-D; 1:1,000 dilution. Mouse anti-Histone H4; Western; abcam; ab10158; 1:1,000 dilution. Mouse anti-RpS25 antibody was kindly provided by N. Nakashima (Western; 1:1,000 dilution) [27]. Mouse anti-Me31B was kindly provided by A. Nakamura (Western, Immunostaining; 1:4,000 dilution, 1:400 dilution) [28]. Rat anti-Yki was kindly provided by H. McNeill (Western; 1:2,000 dilution) [29].

Fly strains

Fly stocks were raised on medium containing 5% corn flour, 4% dry yeast, 3% rice bran, 10% glucose and 0.65% agar at 25°C except for instances where *GMR*-GAL4 driven expression was increased by transfer to 28°C.

Transgenic flies and crosses

Transgenic flies were obtained by P element-mediated germline transformation, and selec-

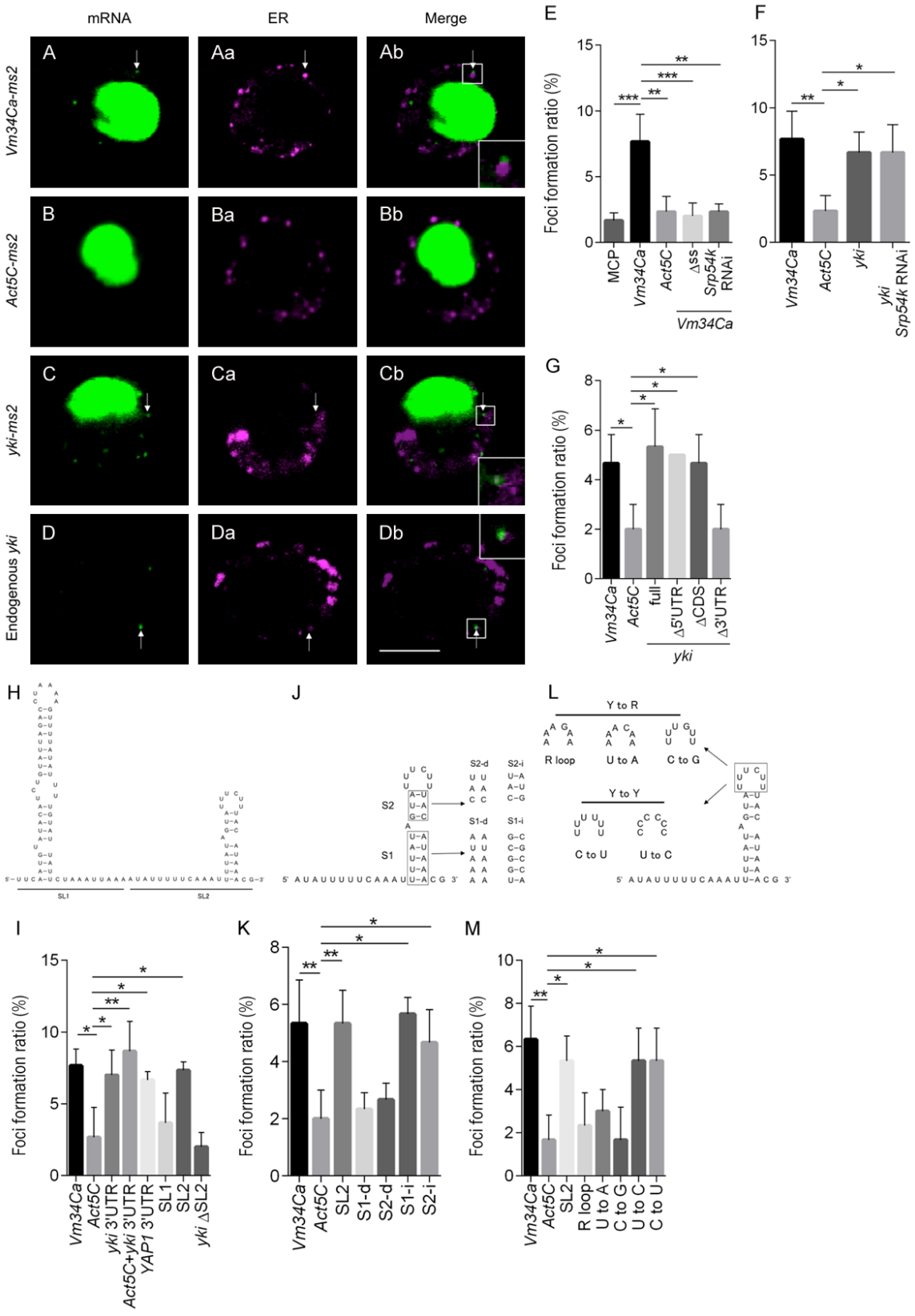

Figure 3. *yki* mRNA forms foci in S2-DRSC cells in the vicinity of the ER via the SL2 motif in the *yki* 3'UTR. (A-D) Subcellular RNA localization. (Aa-Da) The ER is marked by ss-DsRed-HDEL. Scale bar, 5 μm. S2-DRSC cells expressing

target-ms2 RNA, NLS-MCP-GFP and ss-DsRed-HDEL (A-C) were analyzed by confocal microscopy. While *Vm34Ca-ms2* (A-Ab) and *yki-ms2* (C-Cb) RNA form foci (arrow), *Act5C-ms2* RNA (B-Bb) rarely forms foci. ss-DsRed-HDEL marks ER. NLS = nuclear localization signal; ss = signal sequence; HDEL = ER retention signal. (D-Db) Endogenous *yki* mRNA and ER are detected by *in situ* hybridization and anti-KDEL antibody immunostaining, respectively. (Ab-Db) RNA foci are localized adjacent to the ER (white rectangle is magnified in inset, bottom right). (E-G, I, K, M) The foci formation ratio was calculated from the number of cells forming foci in the cytoplasm to the total number of cells expressing GFP in the nucleus. Data are shown as means ± SD (n = 3). (E) *Vm34Ca* and *Act5C-ms2* RNAs were used as positive and negative controls, respectively. *Vm34Ca-ms2* RNA produces foci in an SRP-dependent manner. (F, G) The *yki-ms2* RNA also forms foci efficiently, but in an SRP-independent, and 3'UTR-dependent manner. (H, I) SL2 in the *yki* 3'UTR is necessary for foci formation. (H) Predicted secondary structure of the *yki* 3'UTR: SL1 = stem loop1; SL2 = stem loop2. (J-M) The structure of the SL2 stem regions and pyrimidines in the loop region are critical for foci formation. R = purine; Y = pyrimidine. (J) S1-d and S2-d mutations in SL2 are intended to disrupt secondary structure, while S1-i and S2-i mutations are not. (K) High foci formation ratio is dependent on SL2 secondary structure. (L) Bases in the loop region were exchanged from pyrimidine to purine or from pyrimidine to pyrimidine. (M) The introduction of purines in the loop region decreases foci formation. Data are shown as means ± SD (n = 3). *P<0.05, **P<0.01, ***P<0.001 (one-way ANOVA, Dunnett's Multiple comparisons test).

tion of w^+ flies. Several independent lines for each transgene were established. Transgenic flies were crossed to *GMR*-GAL4 flies to induce expression in eyes, which were subsequently inspected under a scanning electron microscope in high vacuum mode (Keyence VE-7800).

Results

Identification of mRNAs fractionated into microsome fraction in SRP-independent manner

First, to identify mRNAs targeted to rough microsomes (RM) in cultured cells, we performed centrifugal fractionation of cell components (scheme diagrammed in **Figure 1A**). ER components were enriched within fractions 8-10 of the P10 sucrose gradient and thereby termed RM (**Figure 1C**), while tubulin-containing fractions from S10 (data not shown) were considered to be cytoplasmic fraction (C). To remove mRNAs that are associated with the RM fractions via ribosomes, a portion of RM was treated with puromycin and EDTA in high-salt buffer to generate naked microsome (NM) and stripped ribosome (SR) fractions. The absence of ribosomes in NM is illustrated by Western blot analysis using anti-RpS25 antibody (**Figure 1D**).

RNAs fractionated into the RM, C, NM and SR fractions were then identified by deep sequencing. As illustrated in **Figure 2A**, similar numbers of different transcripts were found in the RM and C fractions, and the NM and SR fractions. Although the numbers of transcripts were similar (**Figure 2A**), their compositions were quite different (**Figure 2B**). As expected, Signal peptide prediction using SignalP 4.1 revealed that 81% of the top 200 mRNAs statistics significantly enriched in the soluble C fraction do not harbor canonical signal sequences. Surprisingly though, 78% of the top 200 mRNAs statistics significantly enriched in the NM fraction also do not encode signal peptide- or transmembrane domain-containing proteins. Similar numbers of mRNAs bearing or not bearing signal sequences were found in the RM fraction (**Figure 2B**). Taken together, these data suggest that SRP-independent microsomal targeting mechanisms will have a major impact on the trafficking and translational control of a large percentage and variety of transcripts.

Identification of subcellular localization element in yki mRNA

In order to verify whether the mRNAs biochemically fractionated into NM are localized to the ER in intact cells, we used an MS2 coat protein (MCP) and MCP binding element (ms2) to visualize exogenously expressed transcripts in S2-DRSC cells [30, 31]. As positive and negative controls, we selected RNAs encoded by *Vitelline membrane 34Ca* (*Vm34Ca*), which encodes a secreted protein, and *Actin 5C* (*Act5C*), which encodes a cytoplasmic protein. As expected, these transcripts fractionated primarily into the RM and C fractions, respectively (GSE857-68 dataset). While *Vm34Ca-ms2* RNA formed readily detected foci, *Act5C-ms2* RNA did not (**Figure 3A** and **3B**). Deletion of the predicted signal sequence in *Vm34Ca-ms2* (Δss; **Figure 3E**), reduced the number of detected foci to that of the negative control *Act5C-ms2* (Act5C; **Figure 3E**). A similar reduction in *Vm34Ca-ms2* foci was obtained by knocking down *Signal recognition particle protein 54k* (*Srp54k*), a com-

ponent of the SRP (**Figure 3E**). These data indicate that this imaging system faithfully represents the localization of these transcripts in S2-DRSC cells.

One of the more interesting transcripts that was highly enriched in the ribosome-free NM fraction, and that contains no signal sequence, was that of the Hippo pathway component *yorkie* (*yki*) (**Figure 2C**). Consistent with this enrichment, expression of *yki* mRNA fused to *ms2* tags in S2-DRSC cells resulted in foci formation at a frequency similar to that of *Vm34Ca-ms2* RNA (**Figure 3C** and **3F**). However, in contrast to *Vm34Ca-ms2*, *yki-ms2* foci were not disrupted upon knockdown of *Srp54k* (**Figure 3C** and **3F**). Endogenous *yki* transcripts also formed foci in S2-DRSC cells when examined by *in situ* hybridization (**Figure 3D**). These data show that *yki* mRNA accumulates in microsome-associated foci in an SRP-independent fashion.

To identify cis-elements in the *yki* transcript that mediate foci formation, cells expressing truncated forms of *yki-ms2* RNA were generated. While deletion of the 5'UTR (Δ5'UTR) or coding sequence (ΔCDS) had no effect on foci formation, deletion of the 3'UTR (Δ3'UTR) reduced foci formation to levels similar to the negative control (**Figure 3G**). Furthermore, in cells expressing *yki 3'UTR-ms2* or the *yki* 3'UTR fused to *Act5C-ms2* RNA, foci were formed as efficiently as with the positive control (**Figure 3I**). Taken together, these data indicate that the *yki* 3'UTR is both necessary and sufficient for this type of localization, and that this activity is SRP-independent. Testing the 3'UTR of *YAP1*, the human homolog of *yki*, showed that it was equally efficient at directing the formation of foci (**Figure 3I**), suggesting that the mechanism of foci formation might be conserved from *Drosophila* to humans.

In many cases, cis-elements required for RNA localization have defined secondary structures [16, 32-37]. Secondary structure prediction performed on the *yki* 3'UTR using mfold 3.6 revealed two potential SL structures, SL1 and SL2 (**Figure 3H**). To investigate whether these SLs play a role in *yki* mRNA subcellular localization, ms2-tagged transcripts deleted for either SL1 or SL2 were expressed and examined in S2-DRSC cells. While the SL1-deleted transcripts showed no significant difference, deletion of SL2 (*ΔSL2*) reduced the number of foci to that of the *Act5C* negative control (**Figure 3I**). Further analysis of SL2 was then conducted to determine whether the structure and/or sequence is important for foci formation (**Figure 3J-M**). Base substitutions in either the first (S1-d) or second (S2-d) stem that disrupt base pairing both perturbed foci formation (**Figure 3K**). On the other hand, mutations that alter the stem sequences, while maintaining structure (S1-i, S2-i) had no effect on foci formation (**Figure 3K**). Thus, the secondary structure of the two SL2 stems appears to be their primary contributions to foci formation.

Next, we investigated the role of the loop region (**Figure 3L**). Transversion of pyrimidines to purines extensively reduced foci formation, while transition of pyrimidines to other pyrimidines had no effect (**Figure 3M**). These results show that the loop sequence appears to be critical for localization, but that there is a significant amount of flexibility so long as residues are pyrimidines. Taken together, it appears that the stem structures and loop sequence act together to promote foci formation.

Degradation of yki mRNA through the SL2

As the foci produced by *yki-ms2* RNA are in close proximity to the ER, but did not show a precise overlap (**Figure 3C** and **3Cb**), we examined whether these foci co-localize with other organelles such as Golgi, mitochondria, lysosomes, or cytoplasmic mRNA-protein (mRNP) granules such as processing bodies (P-bodies). The results show that *yki-ms2* foci co-localize with a subset of Me31B (a marker for P-bodies)-containing P-bodies (**Figure 4A** and **4Ab**). This co-localization was also confirmed using double labeling of endogenous *yki* RNA (*in situ* hybridization) together with endogenous Me31B protein (data not shown). Interestingly, *yki* may not require P-bodies to form foci, as knockdown of *HPat* (also known as *Protein associated with topo II related-1*: *Patr-1*), a scaffolding component of P-bodies [38, 39], did not disrupt foci formation (data not shown).

Double labeling with the P-body marker Me31B, and the ER marker KDEL, shows that the P-bodies are detected in the vicinity of ER, but do not appear to overlap precisely with the marker used (**Figure 4B** and **4Bb**). This was also the case with the use of other ER markers (data not shown). Taken together, it appears that the enrichment of *yki* transcripts in micro-

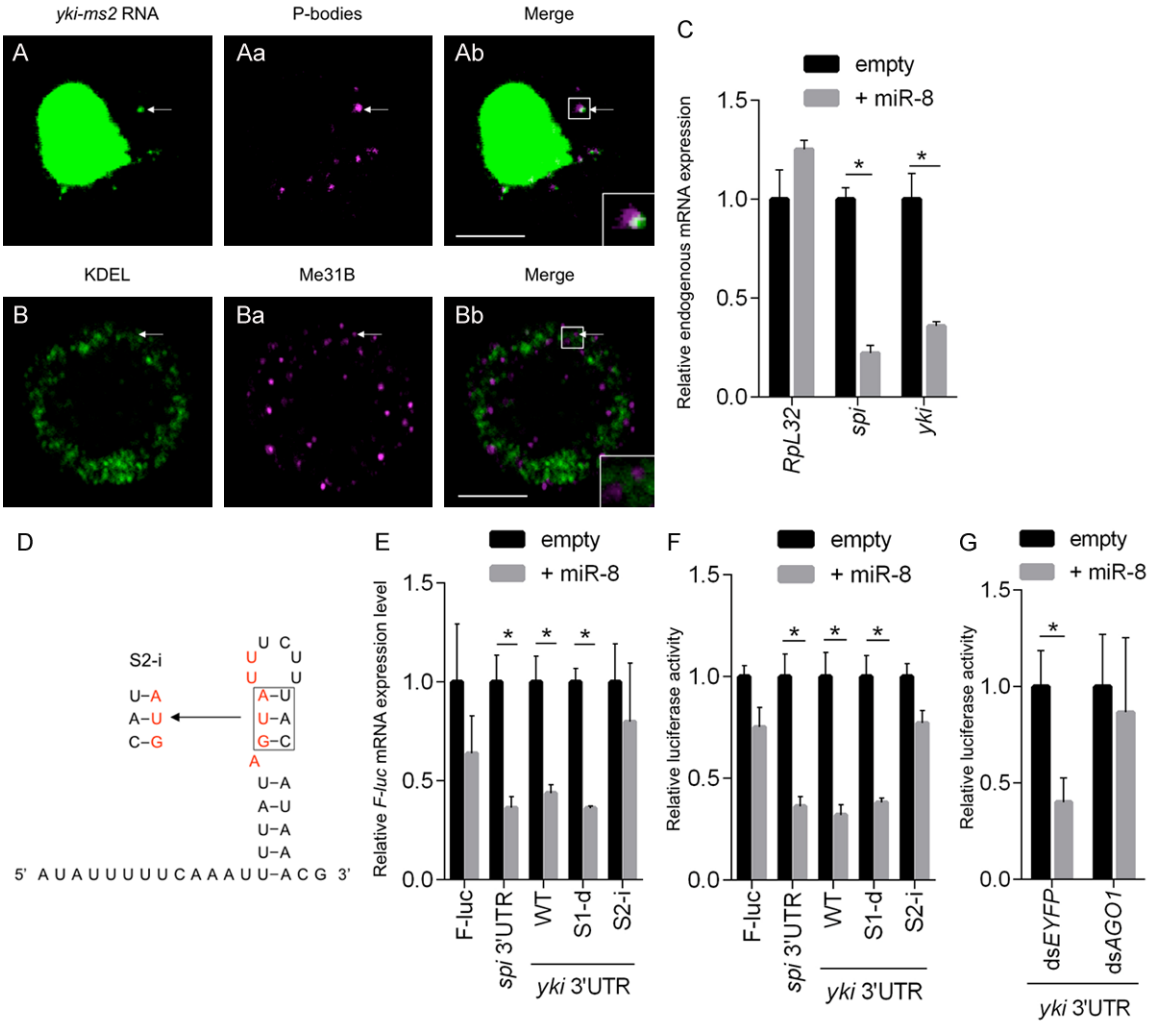

Figure 4. *yki* mRNA is degraded via a *miR-8* seed sequence in the 3'UTR. (A-Ab) *yki-ms2* RNA is partially localized to P-bodies which are represented by Me31B-DsRed. (B-Bb) Endogenous P-bodies detected by anti-Me31B antibody are localized in the vicinity of anti-KDEL ER marker. (C) Expression of endogenous *spi* (positive control) and *yki* mRNAs is decreased in *miR-8*-overexpressing cells, while the amount of *RpL32* mRNA (negative control) is not changed. (D, E) Mutations in the *miR-8* seed sequence (S2-i) disrupt degradation of *F-luc* mRNA bearing the *yki* 3'UTR, but disruption of SL2 stem structure (S1-d) exerts no effect. (D) Schematic of the *miR-8* seed sequence in SL2, and mutation sites of S2-i are shown in red. (E) Relative expression levels of *F-luc* mRNA harboring several variants of the *yki* 3'UTR or *spi* 3'UTR (as positive control) for luciferase based assays. Mutations in the putative *miR-8* seed sequence, such as *S2-i*, perturb the reduction of *F-luc* mRNA in *miR-8* dependent fashion. (F, G) Relative luciferase activity of F-luc harboring several kinds of *yki* 3'UTR or *spi* 3'UTR fusions. (G) In *AGO1*-knockdown cells, *yki* 3'UTR luciferase activity is not repressed. The region marked with white rectangle is magnified in the inset at bottom right. Scale bars, 5 μm (Ab, Bb). Data shown as are means ± SD (n = 3). *P<0.05 (multiple Student's t test) (C, E-G).

somal fractions does not appear to be due to a direct interaction with ER, at least not in the case of detected foci. Rather, it appears to be largely P-body-related. We note, however, that a significant percentage of *yki* transcripts may not be localized to foci, as we were unable to detect non-foci-localized transcripts, either before or after disrupting foci formation (*e.g*; via S2-d mutation).

P-bodies have been shown to regulate both mRNA degradation and translational repression [40, 41]. Consistent with this possible role in regulating *yki*, further analysis of the SL2 sequence revealed the presence of a *miR-8* microRNA seed sequence (**Figure 4D**). To assess the potential regulation of SL2 by *miR-8*, we first measured the level of endogenous *yki* mRNA in a *miR-8*-overexpressing cell line, since

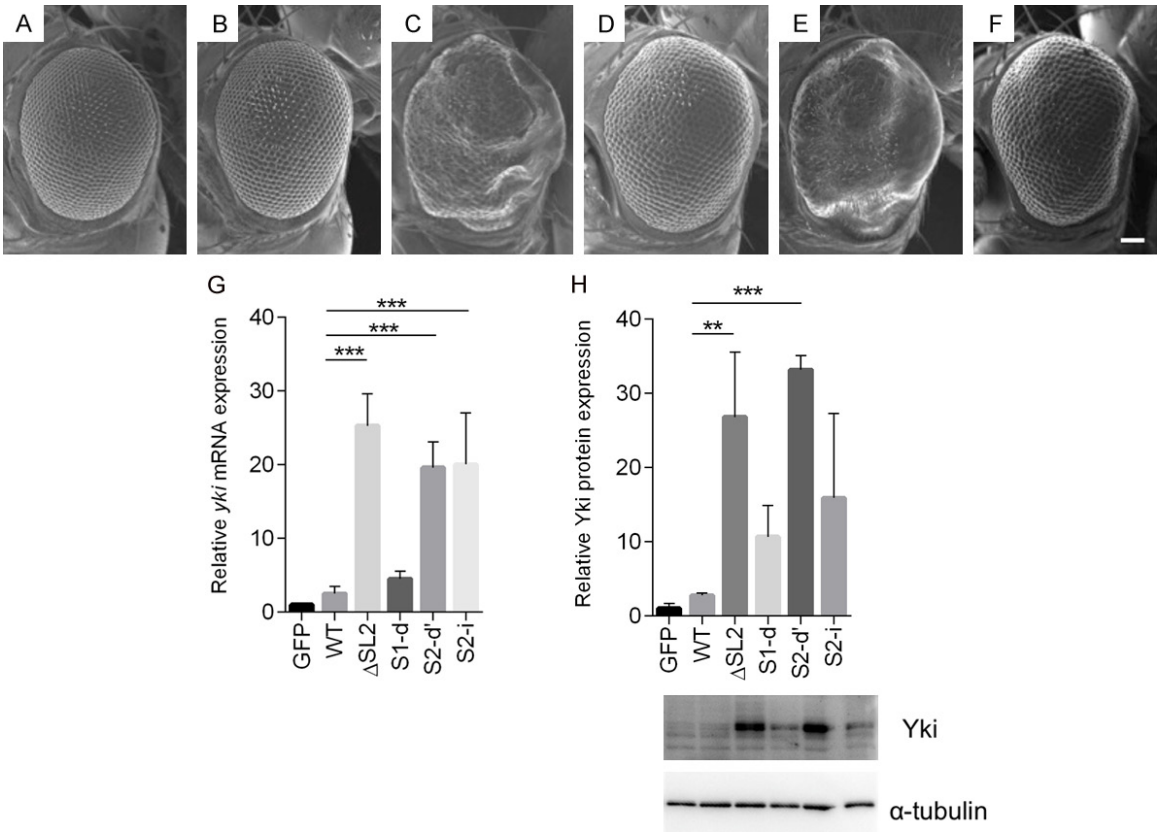

Figure 5. Expression of the ΔSL2 and *S2-d yki* expression constructs in eye discs induces severe rough eye phenotypes. (A-F) Each panel shows a scanning electron micrograph of an adult compound eye. Scale bar, 66.6 μm. (A) *GMR-GAL4/+; UAS-GFP/+; +*, (B) *GMR-GAL4/+; +; UAS-FL (8-1-1)/+*, (C) *GMR-GAL4/UAS-ΔSL2 (20-3-4); +; +*, (D) *GMR-GAL4/+; +; UAS-S1-d (20-3-1)/+*, (E) *GMR-GAL4/+; UAS-S2-d' (84-1)/+; +*, (F) *GMR-GAL4/+; +; UAS-S2-i (13-4)/+*, (G) Relative expression levels of *yki* mRNA in eye imaginal discs, normalised to *GAPDH* mRNA. Transcripts with a missing or disrupted *miR-8* seed sequence over-accumulate (H) Relative Yki protein expression levels normalised to a-tubulin protein expression in eye imaginal discs calculated from Western blots. Level of Yki protein in *S2-d* or *ΔSL2* discs is much higher than controls, while *S1-d* or *S2-i* discs yield moderately increases Yki protein expression. Data are shown as means ± SD (n = 3). **P<0.01, ***P<0.001 (one-way ANOVA, Dunnett's Multiple comparisons test).

S2 cells do not express *miR-8* endogenously [42, 43]. The data clearly show that endogenous *yki* mRNA is specifically and significantly reduced in the presence of *miR-8* (**Figure 4C**). In addition, we examined the relative expression levels of luciferase mRNA reporters fused to *yki* 3'UTRs carrying base substitution mutations in the putative *miR-8* seed sequence that do not disrupt the SL2 distal stem-loop structure (*e.g*; S2-i; **Figure 4E**, and data not shown). The results show that the effects of *miR-8* are clearly dependent on the presence of the *miR-8* seed sequence (**Figure 4F**). This dependence was further validated by showing that knockdown of the RISC complex component *Argonaute-1* (*AGO1*) reverses the effects of *miR-8* ectopic expression (**Figure 4G**).

Biological significance of regulations of yki gene expression at mRNA level

To investigate the biological significance of the SL2 motif on *yki* gene function *in vivo*, we generated transgenic fly lines in which full-length (*FL*), *ΔSL2*, *S1-d*, *S2-d'* and *S2-i yki* transcripts can be ectopically expressed using the GAL4/UAS system. While overexpression of the *FL* construct in eye imaginal discs did not induce any morphological aberrations (**Figure 5B**), expression of the *ΔSL2* variant led to the production of severely enlarged eyes (**Figure 5C**), similar to those previously seen upon expression of non-phosphorylatable Yki [44-46]. Similarly, ectopic expression of *S2-d',* which disrupts both the SL2 distal stem structure and

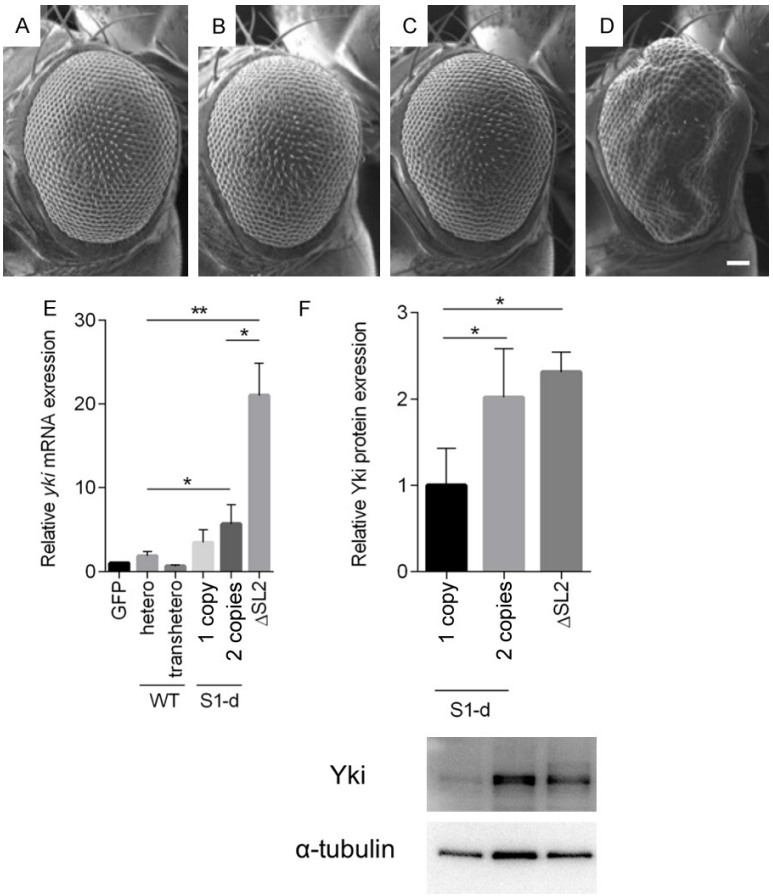

Figure 6. Rough eye phenotypes are enhanced in proportion to the number of copies of UAS-S1-d but not UAS-FL. A-D. In homozygous *FL* expressing flies, eye morphology is the same as in heterozygotes. In contrast, the rough eye phenotype in *S1-d* heterozygotes is enhanced in heteroallelic combinations. A-D. Each panel shows a scanning electron micrograph of an adult compound eye. A-D. Scale bar, 66.6 μm. A. *GMR-GAL4/+; UAS-GFP/+; UAS-yki FL (8-1-1)/+*, B. *GMR-GAL4/+; +; UAS-FL (8-1-1)*, C. *GMR-GAL4/+; UAS-GFP/+; UAS-S1-d (18-3-1)/+*, D. *GMR-GAL4/+; +; UAS-S1-d (18-3-1)/(20-3-1)*, E. Relative expression levels of *yki* mRNA normalised to *GAPDH* mRNA. The relative expression levels of *yki* mRNA in flies carrying 1 copy and 2 copies of *UAS-S1-d* are not significantly different. F. Yki protein is significantly increased in fly carrying 2 copies of *UAS-S1-d*, yielding similar levels of protein as produced by fly carrying 1 copy of UAS-ΔSL2. Data are means SD (n = 3). *P<0.05, **P<0.01 (one-way ANOVA, Dunnetts Multiple comparisons test).

the putative *miR-8* seed sequence, and changes some pyrimidine bases to purine bases in the loop region, also showed dramatic overgrowth (**Figure 5E**). Disruption of just the proximal stem structure (*S1-d*), or just the *miR-8* seed sequence (*S2-i*), had more modest effects (**Figure 5D** and **5F**). These phenotypes were further enhanced by increasing the number of mutated transgene copies from one to two (**Figure 6**). The combined effect of disrupting both stem structure and *miR-8* seed sequence on eye development reveals that both have important contributions to *yki* gene expression and eye development. Similar effects on the growth of legs and wings were observed upon ectopic expression of these constructs using a *dpp*-GAL4 driver (data not shown).

Next we measured the expression levels of *yki* mRNA and Yki protein in the eye imaginal discs of the lines described above (**Figure 5G** and **5H**). Consistent with the results described above, the levels of *yki* mRNA and protein generated by the *FL* construct were not much higher than in control eye imaginal discs. As might be expected from their effects on the *miR-8* seed consensus, the S2-d and S2-i mutations caused similar increases in *yki* RNA stability to that caused by the complete SL2 deletion. However, despite these similarly increased levels of transcript, disruption of just the *miR-8* recognition element (S2-i) did not lead to accumulation of the same amounts of protein as disruption of both the sequence and stem (S2-d), indicating that these elements are selective regulators of stability and translation respectively. The resulting levels of proteins correlate well with the phenotypes rendered by the respective constructs (**Figures 5** and **6**). The relative effects of S2 mutations *in vivo* also correlate well with those observed in S2-DRSC cells.

Discussion

We have shown that a large fraction of transcripts that do not encode transmembrane or secreted proteins associate with microsomes in a non-ribosome-dependent fashion. This includes *yki* transcripts, which fractionated into microsomal fractions SRP-independently, and which colocalize with P-bodies in the vicinity of ER. The correlation between foci localization and translational repression suggests that

these activities are related. Although the proximity of P-bodies to ER has been reported in several organisms [47-55], the biological meaning or origin of this proximity is still unknown. Taken together, our results showing that the human *YAP1* 3'UTR also mediates foci formation (**Figure 3I**), and recent results showing that YAP1 integrates Hippo and unfolded protein responses while controlling liver size and tumorigenesis [56], suggest potentially conserved roles in 3'UTR-mediated post-transcriptional regulatory mechanisms and links to ER stress.

For the P-bodies localization of *yki* mRNA, we indicated that the pyrimidine bases in the loop is necessary in addition to stem structure in SL2. Consistent with our data, recent study revealed that pyrimidine bases in the loop of stem-loop in the *importin β1* 3'UTR is important for its axon localization in mammals [57]. Furthermore, Perry R.B. *et al*. also reported that Nucleolin, mammalian homolog of *Drosophila* modulo, binds to the pyrimidine bases and regulates the axon localization of *importin β1* mRNA. Meanwhile, the other studies have revealed that polypyrimidine tract-binding protein (PTB)/hnRNP I binds to polypyrimidine bases and regulates the subcellular localization or translation of target mRNA in both *C. elegance* and *Drosophila* [58, 59] and that PTB1 and 2, *Arabidopsis thaliana* homologs of PTB, are localized to P-bodies [60]. These data suggest that although the factor(s) that regulates foci formation and translational repression of *yki* mRNA appear to be P-body related, they are yet to be identified.

This study is the first to demonstrate regulation of a Hippo pathway component at the level of RNA post-transcriptional regulation. We have shown that *yki* gene expression is tightly regulated by a single SL structure in the 3'UTR that has the ability to control transcript localization, RNA stability and translation. While there is a strong correlation between foci formation and translational repression, it seems that RNA degradation occurs independently via *miR-8* binding to the corresponding seed sequence in SL2. In the case of *miR-8*, it is expressed in a complex pattern in numerous stages and tissues including the embryo, and larval brain, wing and leg imaginal discs [61]. Thus, it appears that the fate of *yki* mRNA depends on multiple trans-acting factors, each recognizing distinct aspects of SL2 sequence and structure.

Acknowledgements

We are very grateful to E.R. Gavis, N. Nakashima, A. Nakamura and H. McNeill for providing reagents, K. Usui for technical assistance and A. Ephrussi for helpful discussions. We also thank the *Drosophila* Genomics Resource Center for providing the NIH 2P40OD0-10949-10A cultured cell line. RNA-seq analysis was performed in the Cooperative Research Project Program of the Medical Institute of Bioregulation, Kyushu University. This work was supported in part by grants to H.Y. from the Suzuken Memorial Foundation, The Uehara Memorial Foundation, Takeda Science Foundation, Inamori Foundation, Japan Society for the Promotion of Science (JSPS) (Grant Number 26440097) and the JSPS Core-to-Core Program, Asia-Africa Science Platforms, to H.M.K. by the Canadian Institutes of Health Research, and to T.U from The Japan Science Society.

Disclosure of conflict of interest

None.

Authors' contribution

T.U., H.Y., H.K., M.Y., Y.O., T.S., M.I. and M.S. performed experiments and data analysis, H.Y., H.M.K. and M.Y. designed the research, and T. U., H.Y. and H.M.K. wrote the manuscript.

Address correspondence to: Hideki Yoshida, The Center for Advanced Insect Research Promotion, Kyoto Institute of Technology, Matsugasaki, Sakyo-ku, Kyoto 606-8585, Japan. E-mail: hyoshida@kit.ac.jp

References

[1] Huang J, Wu S, Barrera J, Matthews K and Pan D. The Hippo signaling pathway coordinately regulates cell proliferation and apoptosis by inactivating Yorkie, the *Drosophila* Homolog of YAP. Cell 2005; 122: 421-434.

[2] Dong J, Feldmann G, Huang J, Wu S, Zhang N, Comerford SA, Gayyed MF, Anders RA, Maitra A and Pan D. Elucidation of a universal size-control mechanism in *Drosophila* and mammals. Cell 2007; 130: 1120-1133.

[3] Oh H and Irvine KD. *In vivo* regulation of Yorkie phosphorylation and localization. Development 2008; 135: 1081-1088.
[4] Harvey KF, Zhang X and Thomas DM. The Hippo pathway and human cancer. Nat Rev Cancer 2013; 13: 246–257.
[5] Overholtzer M, Zhang J, Smolen GA, Muir B, Li W, Sgroi DC, Deng CX, Brugge JS and Haber DA. Transforming properties of YAP, a candidate oncogene on the chromosome 11q22 amplicon. Proc Natl Acad Sci U S A 2006; 103: 12405-12410.
[6] Zender L, Spector MS, Xue W, Flemming P, Cordon-Cardo C, Silke J, Fan ST, Luk JM, Wigler M, Hannon GJ, Mu D, Lucito R, Powers S and Lowe SW. Identification and validation of oncogenes in liver cancer using an integrative oncogenomic approach. Cell 2006; 125: 1253-1267.
[7] Christensen LL, Holm A, Rantala J, Kallioniemi O, Rasmussen MH, Ostenfeld MS, Dagnaes-Hansen F, Øster B, Schepeler T and Tobiasen H. Functional screening identifies miRNAs influencing apoptosis and proliferation in colorectal cancer. PLoS One 2014; 9: e96767.
[8] Blobel G and Dobberstein B. Transfer of proteins across membranes. I. Presence of proteolytically processed and unprocessed nascent immunoglobulin light chains on membrane-bound ribosomes of murine myeloma. J Cell Biol 1975; 67: 835-851.
[9] Walter P and Blobel G. Translocation of proteins across the endoplasmic reticulum. II. Signal recognition protein (SRP) mediates the selective binding to microsomal membranes of in-vitro-assembled polysomes synthesizing secretory protein. J Cell Biol 1981; 91: 551-556.
[10] Walter P and Johnson AE. Signal sequence recognition and protein targeting to the endoplasmic reticulum membrane. Annu Rev Cell Biol 1994; 10: 87-119.
[11] Diehn M, Bhattacharya R, Botstein D and Brown PO. Genome-scale identification of membrane-associated human mRNAs. PLoS Genet 2006; 2: e11.
[12] Diehn M, Eisen MB, Botstein D and Brown PO. Large-scale identification of secreted and membrane-associated gene products using DNA microarrays. Nat Genet 2000; 25: 58-62.
[13] Lerner RS, Seiser RM, Zheng T, Lager PJ, Reedy MC, Keene JD and Nicchitta CV. Partitioning and translation of mRNAs encoding soluble proteins on membrane-bound ribosomes. RNA 2003; 9: 1123-1137.
[14] Pyhtila B, Zheng T, Lager PJ, Keene JD, Reedy MC and Nicchitta CV. Signal sequence- and translation-independent mRNA localization to the endoplasmic reticulum. RNA 2008; 14: 445-453.
[15] Reid DW and Nicchitta CV. Primary role for endoplasmic reticulum-bound ribosomes in cellular translation identified by ribosome profiling. J Biol Chem 2012; 287: 5518-5527.
[16] Kraut-Cohen J and Gerst JE. Addressing mRNAs to the ER: cis sequences act up! Trends Biochem Sci 2010; 35: 459-469.
[17] Cui XA, Zhang H and Palazzo AF. p180 promotes the ribosome-independent localization of a subset of mRNA to the endoplasmic reticulum. PLoS Biol 2012; 10: e1001336.
[18] Forrest KM and Gavis ER. Live Imaging of Endogenous RNA Reveals a Diffusion and Entrapment Mechanism for nanos mRNA Localization in *Drosophila*. Curr Biol 2003; 13: 1159-1168.
[19] Stark A, Brennecke J, Bushati N, Russell RB and Cohen SM. Animal MicroRNAs confer robustness to gene expression and have a significant impact on 3'UTR evolution. Cell 2005; 123: 1133-1146.
[20] Rehwinkel J, Behm-Ansmant I, Gatfield D and Izaurralde E. A crucial role for GW182 and the DCP1:DCP2 decapping complex in miRNA-mediated gene silencing. RNA 2005; 11: 1640-1647.
[21] Clemens JC, Worby CA, Simonson-Leff N, Muda M, Maehama T, Hemmings BA and Dixon JE. Use of double-stranded RNA interference in *Drosophila* cell lines to dissect signal transduction pathways. Proc Natl Acad Sci U S A 2000; 97: 6499-6503.
[22] Lande MA, Adesnik M, Sumida M, Tashiro Y and Sabatini DD. Direct association of messenger RNA with microsomal membranes in human diploid fibroblasts. J Cell Biol 1975; 65: 513-528.
[23] Sone M, Hayashi T, Tarui H, Agata K, Takeichi M and Nakagawa S. The mRNA-like noncoding RNA Gomafu constitutes a novel nuclear domain in a subset of neurons. J Cell Sci 2007; 120: 2498-2506.
[24] Schleich S, Strassburger K, Janiesch PC, Koledachkina T, Miller KK, Haneke K, Cheng YS, Küchler K, Stoecklin G, Duncan KE and Teleman AA. DENR-MCT-1 promotes translation re-initiation downstream of uORFs to control tissue growth. Nature 2014; 512: 208-212.
[25] Trapnell C, Pachter L and Salzberg SL. TopHat: discovering splice junctions with RNA-Seq. Bioinforma Oxf Engl 2009; 25: 1105-1111.
[26] Trapnell C, Hendrickson DG, Sauvageau M, Goff L, Rinn JL and Pachter L. Differential analysis of gene regulation at transcript resolution with RNA-seq. Nat Biotechnol 2013; 31: 46-53.
[27] Nishiyama T, Yamamoto H, Uchiumi T and Nakashima N. Eukaryotic ribosomal protein

RPS25 interacts with the conserved loop region in a dicistroviral intergenic internal ribosome entry site. Nucleic Acids Res 2007; 35: 1514-1521.

[28] Nakamura A, Amikura R, Hanyu K and Kobayashi S. Me31B silences translation of oocyte-localizing RNAs through the formation of cytoplasmic RNP complex during *Drosophila* oogenesis. Development 2001; 128: 3233-3242.

[29] Badouel C, Gardano L, Amin N, Garg A, Rosenfeld R, Le Bihan T and McNeill H. The FERM-domain protein Expanded regulates Hippo pathway activity via direct interactions with the transcriptional activator Yorkie. Dev Cell 2009; 16: 411-16420.

[30] Bertrand E, Chartrand P, Schaefer M, Shenoy SM, Singer RH and Long RM. Localization of ASH1 mRNA particles in living yeast. Mol Cell 1998; 2: 437-445.

[31] Querido E and Chartrand P. Using fluorescent proteins to study mRNA trafficking in living cells. Methods Cell Biol 2008; 85: 273-292.

[32] Serano TL and Cohen RS. A small predicted stem-loop structure mediates oocyte localization of *Drosophila K10* mRNA. Development 1995; 121: 3809-3818.

[33] Bullock SL, Zicha D and Ish-Horowicz D. The *Drosophila hairy* RNA localization signal modulates the kinetics of cytoplasmic mRNA transport. EMBO J 2003; 22: 2484-2494.

[34] Aragón T, van Anken E, Pincus D, Serafimova IM, Korennykh AV, Rubio CA and Walter P. Messenger RNA targeting to endoplasmic reticulum stress signalling sites. Nature 2009; 457: 736-740.

[35] dos Santos G, Simmonds AJ and Krause HM. A stem-loop structure in the wingless transcript defines a consensus motif for apical RNA transport. Development 2008; 135: 133-143.

[36] Olivier C, Poirier G, Gendron P, Boisgontier A, Major F and Chartrand P. Identification of a conserved RNA motif essential for She2p recognition and mRNA localization to the yeast bud. Mol Cell Biol 2005; 25: 4752-4766.

[37] Cohen RS, Zhang S and Dollar GL. The positional, structural, and sequence requirements of the *Drosophila TLS* RNA localization element. RNA 2005; 11: 1017-1029.

[38] Eulalio A, Behm-Ansmant I, Schweizer D and Izaurralde E. P-body formation is a consequence, not the cause, of RNA-mediated gene silencing. Mol Cell Biol 2007; 27: 3970-3981.

[39] Pradhan SJ, Nesler KR, Rosen SF, Kato Y, Nakamura A, Ramaswami M and Barbee SA. The conserved P body component HPat/Pat1 negatively regulates synaptic terminal growth at the larval *Drosophila* neuromuscular junction. J Cell Sci 2012; 125: 6105-6116.

[40] Behm-Ansmant I, Rehwinkel J, Doerks T, Stark A, Bork P and Izaurralde E. mRNA degradation by miRNAs and GW182 requires both CCR4: NOT deadenylase and DCP1:DCP2 decapping complexes. Genes Dev 2006; 20: 1885-1898.

[41] Coller J and Parker R. General translational repression by activators of mRNA decapping. Cell 2005; 122: 875-886.

[42] Lagos-Quintana M, Rauhut R, Lendeckel W and Tuschl T. Identification of novel genes coding for small expressed RNAs. Science 2001; 294: 853-858.

[43] Ruby JG, Stark A, Johnston WK, Kellis M, Bartel DP and Lai EC. Evolution, biogenesis, expression, and target predictions of a substantially expanded set of *Drosophila* microRNAs. Genome Res 2007; 17: 1850-1864.

[44] Zhang L, Ren F, Zhang Q, Chen Y, Wang B and Jiang J. The TEAD/TEF family of transcription factor Scalloped mediates Hippo signaling in organ size control. Dev Cell 2008; 14: 377-387.

[45] Oh H and Irvine KD. *In vivo* analysis of Yorkie phosphorylation sites. Oncogene 2009; 28: 1916-1927.

[46] Ren F, Zhang L and Jiang J. Hippo signaling regulates Yorkie nuclear localization and activity through 14-3-3 dependent and independent mechanisms. Dev Biol 2010; 337: 303-312.

[47] Nelson KK and Lemmon SK. Suppressors of clathrin deficiency: overexpression of ubiquitin rescues lethal strains of clathrin-deficient Saccharomyces cerevisiae. Mol Cell Biol 1993; 13: 521-532.

[48] Wilhelm JE, Buszczak M and Sayles S. Efficient protein trafficking requires trailer hitch, a component of a ribonucleoprotein complex localized to the ER in *Drosophila*. Dev Cell 2005; 9: 675-685.

[49] Decker CJ and Parker R. CAR-1 and trailer hitch: driving mRNP granule function at the ER? J Cell Biol 2006; 173: 159-163.

[50] Beckham CJ, Light HR, Nissan TA, Ahlquist P, Parker R and Noueiry A. Interactions between brome mosaic virus RNAs and cytoplasmic processing bodies. J Virol 2007; 81: 9759-9768.

[51] Squirrell JM, Eggers ZT, Luedke N, Saari B, Grimson A, Lyons GE, Anderson P and White JG. CAR-1, a protein that localizes with the mRNA decapping component DCAP-1, is required for cytokinesis and ER organization in Caenorhabditis elegans embryos. Mol Biol Cell 2006; 17: 336-344.

[52] Thomson T, Liu N, Arkov A, Lehmann R and Lasko P. Isolation of new polar granule components in *Drosophila* reveals P body and ER associated proteins. Mech Dev 2008; 125: 865-873.

[53] Kilchert C, Weidner J, Prescianotto-Baschong C and Spang A. Defects in the secretory pathway and high Ca2+ induce multiple P-bodies. Mol Biol Cell 2010; 21: 2624-2638.
[54] Weil TT, Parton RM, Herpers B, Soetaert J, Veenendaal T, Xanthakis D, Dobbie IM, Halstead JM, Hayashi R, Rabouille C and Davis I. *Drosophila* patterning is established by differential association of mRNAs with P bodies. Nat Cell Biol 2012; 14: 1305-1313.
[55] Huch S, Gommlich J, Muppavarapu M, Beckham C and Nissan T. Membrane-association of mRNA decapping factors is independent of stress in budding yeast. Sci Rep 2016; 6: 25477.
[56] Wu H, Wei L, Fan F, Ji S, Zhang S, Geng J, Hong L, Fan X, Chen Q, Tian J, Jiang M, Sun X, Jin C, Yin ZY, Liu Q, Zhang J, Qin F, Lin KH, Yu JS, Deng X, Wang HR, Zhao B, Johnson RL, Chen L and Zhou D. Integration of Hippo signalling and the unfolded protein response to restrain liver overgrowth and tumorigenesis. Nat Commun 2015; 6: 6239.
[57] Perry RB, Rishal I, Doron-Mandel E, Kalinski AL, Medzihradszky KF, Terenzio M, Alber S, Koley S, Lin A, Rozenbaum M, Yudin D, Sahoo PK, Gomes C, Shinder V, Geraisy W, Huebner EA, Woolf CJ, Yaron A, Burlingame AL, Twiss JL and Fainzilber M. Nucleolin-Mediated RNA Localization Regulates Neuron Growth and Cycling Cell Size. Cell Rep 2016; 16: 1664-1676.
[58] Besse F, López de Quinto S, Marchand V, Trucco A and Ephrussi A. *Drosophila* PTB promotes formation of high-order RNP particles and represses oskar translation. Genes Dev 2009; 23: 195-207.
[59] Cote CA, Gautreau D, Denegre JM, Kress TL, Terry NA and Mowry KL. A Xenopus protein related to hnRNP I has a role in cytoplasmic RNA localization. Mol Cell 1999; 4: 431-437.
[60] Stauffer E, Westermann A, Wagner G and Wachter A. Polypyrimidine tract-binding protein homologues from Arabidopsis underlie regulatory circuits based on alternative splicing and downstream control. Plant J Cell Mol Biol 2010; 64: 243-255.
[61] Karres JS, Hilgers V, Carrera I, Treisman J and Cohen SM. The conserved microRNA miR-8 tunes atrophin levels to prevent neurodegeneration in *Drosophila*. Cell 2007; 131: 136-145.